Anisotropy of the electronic g factors for anomalous muonium in silicon and germanium

K. W. Blazey
IBM Zurich Research Laboratory, CH-8803 Rüschlikon, Switzerland

T. L. Estle
Rice University, Houston, Texas 77251

E. Holzschuh, P. F. Meier, B. D. Patterson, and M. Richner
Physikalisches Institut, Universität Zürich, CH-8001 Zurich, Switzerland

(Received 6 August 1985)

When the electronic g factor is isotropic, one of the muon-spin-rotation (μSR) frequencies of anomalous muonium is almost isotropic at a particular value of the applied magnetic field, the magic field. By measuring the field dependence of the μSR frequencies around this magic field, the g-factor anisotropy $g_{\|}-g_{\perp}$ in Ge is found to be $+0.0330(12)$ while that in Si is zero $[+0.0002(8)]$ within experimental accuracy. The consequences of these results for a model of anomalous muonium are discussed in terms of the g-factor anisotropies for known defects in Si.

I. INTRODUCTION

Muon-spin-rotation (μSR) experiments in crystals of diamond, silicon, and germanium have revealed the existence of two muonium-like centers when positive muons are stopped in these crystals.[1] These two centers are referred to as normal muonium (Mu), which has an isotropic hyperfine interaction about one-half the free-muonium value, and anomalous muonium (Mu*), which is quite unlike muonium in vacuum. Anomalous muonium has a highly anisotropic hyperfine interaction which is only a few percent of the free-muonium value and which has axial symmetry about one of the crystalline $\langle 111 \rangle$ axes.

Experiments on Mu* have not yet provided sufficient information to permit the structure of anomalous muonium to be inferred. In the search for additional experimental evidence which might be useful in determining a model for the center, we have undertaken a study of the electronic g factors of anomalous muonium in silicon and germanium.[2] Muon-spin-rotation experiments on anomalous muonium are normally rather insensitive to the electronic g factors because the frequencies observed are magnetic dipole transitions of the muon spin, and at high field Mu* is in the Paschen-Back regime. However, there are two situations in which the electronic g factors make a more significant contribution to the observations. At low applied magnetic fields, there is a small dependence of the μSR frequencies upon the g factors. This is masked as the field is lowered by the increased linewidth and accompanying frequency shifts of the μSR lines because of nuclear hyperfine interactions.[3] In addition, at fields near the so-called "magic field," the small dependence of the μSR frequencies upon the anisotropy of the g factor is most evident. It is this last phenomenon which we exploit in this paper.

The precessional frequencies of the muon spin in Mu* at high fields may be considered to result from precession in an effective field which is the vector sum of the applied and hyperfine fields.[4] The latter is anisotropic and it has different values for the two electron-spin states. If the magnitude of the effective field is the same for the field applied parallel and perpendicular to the $\langle 111 \rangle$ symmetry axis, then the magnitude of the effective field will be independent of the orientation of the applied field. The value of the applied field at which this occurs is the (first-order) magic field. The applied field and the effective field are parallel when the applied field is along the direction of the larger of $|A_{\|}|$ and $|A_{\perp}|$. They are antiparallel when the applied field is along the direction of the smaller of $|A_{\|}|$ and $|A_{\perp}|$. By varying the magnitude of the applied field near the magic field, the lower-frequency μSR lines of all the differently oriented Mu* centers will cross at a single value of the field. The approximate values [see Eq. (5)] of the magic fields for Mu* in Si and Ge are 0.2018 and 0.2920 T, respectively, so that the high-field approximation used in this description is good (i.e., $|A_{\perp}|/2\mu_B H$ is 0.0164 and 0.0159, respectively).

Implicit in this description is the isotropy of the electronic g factor. If the electronic g factor is anisotropic, then there is no field at which any μSR line is independent of angle. Consequently, if the g factor is not isotropic, then there will be no single crossing of the μSR lines from the differently oriented Mu* centers as the field is varied. A quantitative study of this region of near crossing can thus be used to determine the anisotropy of the g factor for Mu*.

The shifts of the principal values of the g factor, $g_{\|}$ and $g_{\perp}$, from the free-electron value of 2.0023 are a measure of the admixture of excited states into the ground state by spin-orbit coupling. Although we only measure $g_{\|}-g_{\perp}$ in this experiment, it can be compared to the theory of the g shifts for centers in crystals. The theory of the g tensor of deep centers in silicon was first studied

by Watkins and Corbett,[5] and, subsequently, by these authors,[6] Phillips,[7] and more recently by Lannoo and Bourgoin.[8] By far the most extensive experimental data on g shifts of defects in semiconductors is that on silicon. In 1973, Lee and Corbett[9] plotted the g shifts of about 40 centers observed in irradiated Si. More recently, Sieverts[10] has given a more systematic discussion of the g shifts for various types of centers in Si. Comparison of these g shifts with those observed for anomalous muonium gives some insight into the nature of Mu*.

In this paper, we discuss the theory of the measurements near the magic field and the theory of the g shifts in Sec. II and describe the experimental techniques in Sec. III. In Sec. IV the results are presented and analyzed, while in Sec. V we discuss the possible implications of these results.

II. THEORY

A. "Magic field"

The spin Hamiltonian describing anomalous muonium is

$$\mathcal{H}=g_{\|}\mu_B H_z S_z+g_{\perp}\mu_B(H_x S_x+H_y S_y)+A_{\|}S_z I_z +A_{\perp}(S_x I_x+S_y I_y)-g_{\mu}\mu_{\mu}\mathbf{H}\cdot\mathbf{I}\,, \tag{1}$$

where the z axis is the particular $\langle 111\rangle$ symmetry axis of the anomalous muonium center under analysis. Anomalous muonium centers are formed with equal probability with each of the four possible $\langle 111\rangle$ symmetry axes. The energy levels and eigenfunctions of this Hamiltonian can readily be determined by diagonalizing the resultant 4×4 matrix. From the eigenvectors and the initial muon polarization ($\sim 100\%$ along the beam axis), the relative amplitudes of the several precessional components can be obtained. We compare these exact results with the experimental data to extract the parameters in the spin Hamiltonian, particularly $g_{\|}-g_{\perp}$. Figure 1 shows the field dependence of the muon precessional frequencies for four different orientations of the applied field in Si assuming $g_{\|}=g_{\perp}$. It is seen that the lower μSR frequencies ν_{43} become equal for all orientations near 0.2 T, the silicon magic field. Near this crossover is the region of interest in this paper.

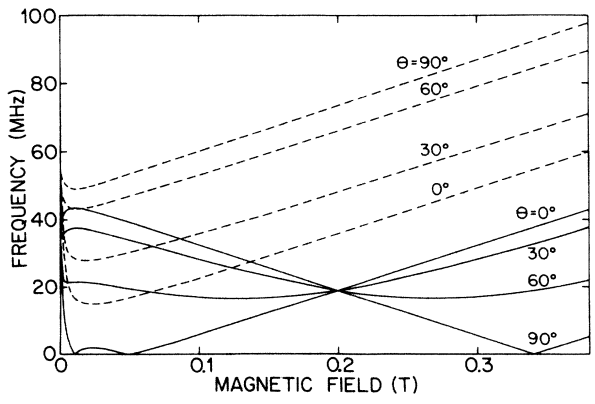

FIG. 1. Calculated variation of the Mu* μSR frequencies of Mu* in Si with applied magnetic field for four different orientations of the magnetic field. Solid line denotes, ν_{43} and dashed line denotes, ν_{12}. The calculations were made assuming that the electronic g factor is isotropic and that $A_{\|}+A_{\perp}>0$.

A better understanding and an analysis valid to better than the experimental uncertainty results from a perturbation treatment valid at high fields. The particular perturbation treatment used is outlined in the Appendix. In Fig. 1 and throughout much of the discussion in this paper, the transitions have been labeled assuming $A_{\|}+A_{\perp}>0$. It is based on the approximation that the electronic Zeeman interaction is much larger than any other term in the spin Hamiltonian, but that the hyperfine interaction and the muon Zeeman interaction are comparable. The results derived in the Appendix are valid to third order, i.e., $O(A^3/(g\mu_B H)^2)$, and are consequently very accurate (the error is less than or of the order of 1 kHz for Mu* in Si for $H\gtrsim 0.1$ T).

The lowest μSR frequency [either ν_{43} in Eq. (A7) or ν_{21} in Eq. (A8)] can be written to first order as[4]

$$h\nu=\left[\left[\frac{A_{\|}}{2}\mp g_{\mu}\mu_{\mu}H\right]^2\cos^2\theta+\left[\frac{A_{\perp}}{2}\mp g_{\mu}\mu_{\mu}H\right]^2\sin^2\theta\right]^{1/2}, \tag{2}$$

provided that $g=g_{\perp}$. By choosing the field so that

$$\left|\frac{A_{\|}}{2}\mp g_{\mu}\mu_{\mu}H\right|=\left|\frac{A_{\perp}}{2}\mp g_{\mu}\mu_{\mu}H\right|, \tag{3}$$

we find that ν is independent of the field direction. This value of the magnetic field is the "magic field" (to first order). Solving Eq. (3), one obtains

$$H_M^{(1)}=\frac{1}{4g_{\mu}\mu_{\mu}}\,|A_{\perp}+A_{\|}|\,. \tag{4}$$

At the magic field, the lowest μSR frequency is to first order

$$h\nu_M^{(1)}=\tfrac{1}{4}\,|A_{\perp}-A_{\|}|\,. \tag{5}$$

Although this analysis is suggestive, the values of the magic field are not high enough to allow the neglect of the second-order terms. Including terms through second order we obtain Eq. (A10) of the Appendix, which may be written as

$$h\nu=h\nu_M^{(2)}+S_1 g_{\mu}\mu_{\mu}(H-H_M^{(2)})\cos(2\theta) -\tfrac{1}{16}S_2(A_{\|}+A_{\perp})\frac{\Delta g}{g_0}[1-\cos(4\theta)]\,. \tag{6}$$

In Eq. (6) the magic field to second order, $H_M^{(2)}$, is given by

$$H_M^{(2)}=\frac{1}{4g_{\mu}\mu_{\mu}}\,|A_{\perp}+A_{\|}|\,(1-\epsilon)\,, \tag{7}$$

and the corresponding μSR frequency by

$$h\nu_M^{(2)}=\tfrac{1}{4}\,|A_{\perp}-A_{\|}|\,(1+\epsilon)\,, \tag{8}$$

where

$$\epsilon=2\frac{g_\mu\mu_\mu}{g_0\mu_B}\frac{A_\perp}{A_{||}+A_\perp}\ .$$

The quantities S_1 and S_2 can be either $+1$ or -1 and are given by

$$S_1=\frac{A_\perp^2-A_{||}^2}{|A_\perp^2-A_{||}^2|}\quad S_2=\frac{A_\perp-A_{||}}{|A_\perp-A_{||}|}\ ,$$

while Δg and g_0 are given by $\Delta g=g_{||}-g_\perp$, $g_0=\frac{1}{3}g_{||}+\frac{2}{3}g_\perp$. The coefficient of $\cos(2\theta)$ can be made zero by setting the applied magnetic field to the magic field. The second-order magic fields of Eq. (7) calculated for $g_0=2$ are 0.2002 and 0.2897 T for silicon and germanium, respectively. In the group-III–V compounds[11] GaAs and GaP the magic fields to second order are 0.5620 and 0.5491 T, respectively, whereas the value for diamond is 0.4073 T. A measurement of the lower μSR frequency as a function of applied field for all Mu* centers will show a crossing at these values of the applied field if Δg is small enough. Because of this phenomenon, the lower μSR frequency has been observed in powdered silicon and diamond at their respective magic fields.[12]

If, however, there is some g-factor anisotropy, the term in $\cos(4\theta)$ is no longer zero and a single crossing of the lower μSR frequencies of all Mu* centers as a function of the applied field will no longer be observed. This deviation from a single crossing is used here to determine the value of the g-factor anisotropy, Δg.

B. The g shifts

The g tensor can be calculated by including in the Hamiltonian the terms which represent the interaction of the electrons with an electromagnetic field. This can be written as

$$\mathscr{H}=g_e\mu_B\mathbf{H}\cdot\mathbf{S}+\frac{\mu_B}{mc}\left[\mathbf{E}\times\left[\mathbf{p}+\frac{e}{c}\mathbf{A}\right]\right]\cdot\mathbf{S}+\frac{e}{2mc}(\mathbf{p}\cdot\mathbf{A}+\mathbf{A}\cdot\mathbf{p})+\frac{e^2}{2mc^2}A^2\ , \tag{9}$$

where there must be such a contribution for each electron. If we assume the ground state can be described by the orbital, $|0\rangle$, of one unpaired electron then we obtain from Eq. (9) the spin Hamiltonian for the electron Zeeman interaction as

$$\mathscr{H}_s=\mu_B\left[g_e\mathbf{H}+\frac{e}{mc^2}\langle 0|\mathbf{E}\times\mathbf{A}|0\rangle-\frac{e}{2m^2c^2}\sum_{n\neq 0}\frac{1}{E_n-E_0}(\langle 0|\mathbf{p}\cdot\mathbf{A}+\mathbf{A}\cdot\mathbf{p}|n\rangle\langle n|\mathbf{E}\times\mathbf{p}|0\rangle+\langle 0|\mathbf{E}\times\mathbf{p}|n\rangle\langle n|\mathbf{p}\cdot\mathbf{A}+\mathbf{A}\cdot\mathbf{p}|0\rangle)\right]\cdot\mathbf{S}\ , \tag{10}$$

where $\mathbf{A}$ is the vector potential and $\mathbf{E}$ the electric field resulting from the charged particles in the crystal. The first-order contribution is usually negligible, and the second-order term will simplify if the ground-state orbital, $|0\rangle$, and the other orbitals, $|n\rangle$, are written as linear combinations of atomic orbitals (LCAO). Then, if overlap is negligible, one obtains the g tensor

$$\underline{g}=g_e\underline{I}-\sum_{i,j}[a_i(0)]^*a_j(0)\sum_{n\neq 0}\frac{a_i(n)[a_j(n)]^*}{E_n-E_0}(\lambda_j\langle i,0|\mathbf{L}_i|i,n\rangle\langle j,n|\mathbf{L}_j|j,0\rangle+\lambda_i\langle j,n|\mathbf{L}_j|j,0\rangle\langle i,0|\mathbf{L}_i|i,n\rangle)\ , \tag{11}$$

where

$$|0\rangle=\sum_i a_i(0)|i,0\rangle,\quad |n\rangle=\sum_i a_i(n)|i,n\rangle\ ,$$

the sum is over the atoms on which a significant electron density exists, and the functions $|i,0\rangle$ and $|i,n\rangle$ are sums of atomic orbitals on the atom i. This version is more general than usually found in the literature because of the possible many-center character of the Mu* ground state. The sum over n includes orbitals both lower and higher in energy, and thus with E_n-E_0 both less than and greater than zero. In addition, the coefficients $a_i(0)$ and $a_i(n)$ may vary in sign. It is consequently very difficult to make any predictions about $g_{||}$ and $g_\perp$ for anomalous muonium. A detailed model of the center, in which the energies and LCAO:MO (where MO denotes molecular orbital) eigenfunctions of all states important in Eq. (11), might permit approximate calculations of $g_{||}$ and $g_\perp$. In the absence of such models, no such calculations are presented here.

The g shifts arise from the spin-orbit coupling, λ, of the silicon or germanium atoms for the crystals studied here. The larger atomic spin-orbit parameter for the valence orbitals of Ge than for those of Si suggests a larger g shift and hence a larger Δg for Ge than for Si. Assuming the other orbitals differ in energy from the ground state by an energy which scales roughly as the band gap from one crystal to the other, then the values of Δg should be approximately in the ratio of λ/E_0, where E_0 is the $k=0$ direct energy gap. Taking $E_0=0.89$ eV for Ge and 4.18 eV for Si (Ref. 13) and the spin-orbit constant $\lambda=0.29$ eV for Ge and 0.044 eV for Si, the ratio of λ/E_0 for Ge and Si is 31. While this gives an idea of the relative size of the g shifts to be expected, neither the sign of Δg nor the signs of $g_{||}-g_e$ or $g_\perp-g_e$ can be predicted.

III. EXPERIMENT

The experiments were performed at the meson facility of the Swiss Institute for Nuclear Research. A pure germanium crystal was obtained from EG&G Ortec, Oak Ridge, with the following order-of-magnitude known im-

purities: [C]$\sim 10^{15}$ cm^{-3}, [Si]$\sim 10^{13}$ cm^{-3}, [O]$\sim 10^{12}-10^{13}$ cm^{-3}, [Ga] and [In]$\sim 10^{9}$ cm^{-3}, [Al]$\sim 2\times 10^{10}$ cm^{-3}, [B] and [P]$\sim 2\times 10^{10}$ cm^{-3}, and [H]$\sim 10^{15}$ cm^{-3}, but some of the hydrogen is subsequently baked out. This crystal was oriented so it could be mounted in a He-gas–flow cryostat with the magnetic field $\mathbf{H}\|\langle 331\rangle$, and the muon beam entering along $\langle \bar{1}093\rangle$ which is also the direction of the muon polarization. In this configuration, two of the four $\langle 111\rangle$ axes make the same angle with the field, while the other two make different angles with the field. Thus, six frequencies arising from Mu* appear in the resultant μSR spectrum with generally good resolution of the three low-frequency lines and with the weakest line stronger than for other possible orientations.

Since the signals in Si are much stronger than in Ge, no attempt was made to optimize the amplitudes, and the magnetic field was applied along $\langle 112\rangle$ with the beam axis along $\langle 11\bar{1}\rangle$. Again, in this configuration Mu* contributes six frequencies to the μSR spectrum. The Si crystal used was B-doped (p type) with 10^{11}-cm^{-3} electrically active impurities ($\rho=450$ to 1000 Ω cm).

The temperature of measurement was 24.5 K for Ge and 21.5 K for Si. Time-differential transverse-field muon-spin-rotation data were collected in four histograms from which the precessional frequencies were extracted by multifrequency fits. Data were taken at several fields around the magic field so that the exact field dependence of ν_{43} could be determined for the three kinds of inequivalent Mu* centers as shown for each crystal in Fig. 2. The deviation from a single crossing of these three branches was attributed to the electronic g-factor anisotropy.

A check on the crystal alignment was obtained from the other Mu* frequencies ν_{21}, that is at higher frequencies. In Ge, there was no indication of any splitting in these lines and therefore $\mathbf{H}$ must lie in a $\{110\}$ plane. The exact location in the $\{110\}$ plane was left a variable of the computer fit of the spin Hamiltonian to the field dependence of all six frequencies. A splitting of the high-frequency lines in Si was observed, and therefore the angle out of the $\{110\}$ plane had to be included as an additional variable when fitting the field dependence of the six μSR frequencies from Mu*.

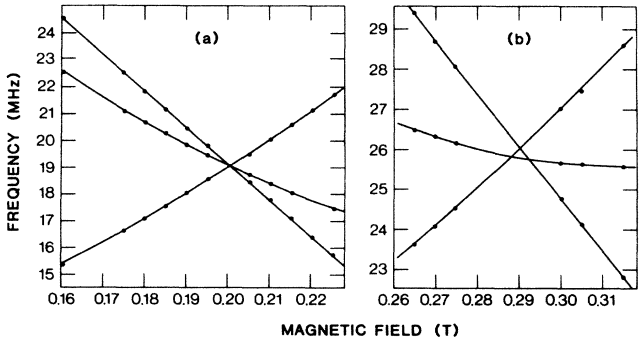

FIG. 2. The measured field dependence of the low-frequency lines, ν_{43} for Mu* in (a) Si and (b) Ge, (Ref. 2).

IV. RESULTS

The variation of the low-frequency μSR lines, ν_{43}, of the three differently oriented anomalous muonium centers with applied magnetic field is plotted for Ge and Si in Fig. 2. It is clear that while the branches almost cross at a single point for Si, they do not for Ge. To obtain the electronic g-factor anisotropy, all six field-dependent frequencies were fit to the numerically determined eigenvalues of the spin Hamiltonian, Eq. (1), using the frequency of precession of bare muons to determine the value of the applied magnetic field.

The values of the spin-Hamiltonian parameters giving the best fit for Ge are

$$g_{\|}-g_{\perp}=0.0330\pm 0.0012\ ,$$

$$g_{\perp}=1.953\pm 0.085\ ,$$

$$g_{\mu}=2.0021\pm 0.0004\ ,$$

$$A_{\|}=27.294\pm 0.022\ ,$$

$$A_{\perp}=130.891\pm 0.013\ ,$$

$$\chi^2=41.25\ ,$$

with 29 degrees of freedom. In the case of Si, the values are

$$g_{\|}-g_{\perp}=0.0002\pm 0.0008\ ,$$

$$g_{\perp}=2.19\pm 0.085\ ,$$

$$g_{\mu}=2.0022\pm 0.0002\ ,$$

$$A_{\|}=16.760\pm 0.014\ ,$$

$$A_{\perp}=92.603\pm 0.005\ ,$$

$$\chi^2=110.27\ ,$$

with 70 degrees of freedom.

These results clearly show an electronic g-factor anisotropy in Ge but not in Si. The error in $g_{\perp}$ makes it compatible with the free-electron g value in Ge, and the large value of $g_{\perp}$ in Si is probably not significant.

V. CONCLUSION

The observation that $g_{\|}-g_{\perp}=0.0330\pm 0.0012$ for anomalous muonium in germanium cannot, by itself, provide much insight into the structure of anomalous muonium. However, when taken together with other information it can be a useful constraint on a model for Mu*. The empirical classification of defects in silicon developed by Lee and Corbett[9] and extended by Sieverts[10] is probably the best guide to the significance of the fact that $g_{\|}>g_{\perp}$. Sieverts classifies defects into four types. In one of these four, $g_{\|}$ is always larger than $g_{\perp}$, in one $g_{\perp}>g_{\|}$, and in the other two $g_{\|}-g_{\perp}$ can have either sign. Thus, on this basis, Mu* in germanium could belong to any of three types.

However, a specific model for anomalous muonium, based on several other observed properties, has been suggested. This model is that anomalous muonium is simply substitutional muonium. Estle[14] suggested this based pri-

marily upon the fact that the contact hyperfine interaction is very small and that Mu* is more stable than normal muonium in diamond. Simple molecular orbital arguments, which are confirmed by a detailed calculation,[15] indicate that substitutional muonium or hydrogen should behave much as a vacancy, i.e., there should be an orbital triplet state in the gap. Similar conclusions have been reached by Patterson *et al.*[16] from channeling measurements of the positrons resulting from muon decay. Theoretically, Das *et al.*[17] have analyzed such a model as have Mainwood and co-workers.[18] If one takes this model seriously, then one should regard Mu* as a defect of the same type as a vacancy, that is, Sieverts' type *B*. Type-*B* defects are those in which $g_{||}$ is always larger than $g_{\perp}$.

Thus, the fact that $g_{||} > g_{\perp}$ for anomalous muonium in Ge would appear to be further support for the model of Mu* as substitutional muonium. However, for Si we have $g_{||} - g_{\perp} = 0$ within experimental accuracy. Although this is reasonable since the spin-orbit interaction in silicon is smaller than in germanium, and the gap is larger, it does demonstrate that the value of $g_{||} - g_{\perp}$ which should be compared to those of type-*B* defects in Si is smaller than for any type-*B* defect in Sieverts' tabulation. In this respect, Mu* in Ge more closely approximates a Sieverts type-*D* defect. The anisotropic defects of this type have smaller values of $|g_{||} - g_{\perp}|$ than do type-*B* defects, and for about half of these $g_{||} > g_{\perp}$. Since type-*D* defects are substitutional or interstitial impurities, this interpretation provides no insight into the μ^+ site in Mu*. The principal difference between the two types is that $g_{||} > g_e$ for type-*B* and $g_{||} \lesssim g_e$ for anisotropic type-*D* defects. An accurate measurement of $g_{||}$ and/or $g_{\perp}$ would help to classify Mu* better according to the empirical classification scheme of Lee, Corbett, and Sieverts, provided that the Sieverts classification scheme can be applied to Ge. Unfortunately, it does not appear that an accurate *g*-value measurement can be made since at low fields, where the μSR frequencies depend more on the electronic *g* factor, nuclear hyperfine interactions broaden and shift the μSR line. An alternate approach, that of measuring the EPR spectrum by the technique known as double-electron muon resonance,[19] did not give accurate electronic *g* factors either because of the large inhomogeneous linewidths of the EPR lines.[20] Thus, it appears that only the value of $g_{||} - g_{\perp}$ for Mu* in Ge will be available to compare with theory, and its utility will be limited. In principal, once a detailed theoretical model exists, the *g* factor could be calculated. In practice, this has been difficult for even the simplest of defects. Consequently, the prospects for reliable calculated *g* values for Mu* in Ge are not good.

ACKNOWLEDGMENT

The work of T. L. Estle was supported by National Science Foundation Grant No. DMR-79-09223.

APPENDIX

The spin Hamiltonian of Eq. (1) can be written in terms of the *g* tensor $\underline{g}$, and the hyperfine tensor $\underline{A}$, as

$$\mathcal{H} = \mu_B \mathbf{H}\cdot\underline{g}\cdot\mathbf{S} + \mathbf{S}\cdot\underline{A}\cdot\mathbf{I} - g_\mu\mu_\mu \mathbf{H}\cdot\mathbf{I} . \tag{A1}$$

Choosing as quantization axis for the electron spin the unit vector $\hat{\xi}$, along $\mathbf{H}\cdot\underline{g}$, we may write Eq. (A1) as

$$\mathcal{H} = g\mu_B H S_\xi + (S_\xi \hat{\xi}\cdot\underline{A} - g_\mu\mu_\mu \mathbf{H})\cdot\mathbf{I} + (S_\xi \hat{\xi} + S_\eta \hat{\eta})\cdot\underline{A}\cdot\mathbf{I} , \tag{A2}$$

where *g* is the angle-dependent *g* factor for axial symmetry, defined in Eq. (A4), and $\hat{\xi}$ and $\hat{\eta}$ are unit vectors normal to $\hat{\zeta}$ and to each other. By quantizing the muon spin along $\pm\frac{1}{2}\hat{\zeta}\cdot\underline{A} - g_\mu\mu_\mu\mathbf{H}$ for the electron-spin state with $M_s = \pm\frac{1}{2}$, one immediately obtains the energies, if terms $\lesssim O(A^2/g\mu_B H)$ can be neglected. These vectors are $-g_\mu\mu_\mu$ times the effective fields acting on the muon spin and consist of the vector sum of the applied and hyperfine fields (see Ref. 4). Using this as the starting point for a third-order perturbation calculation, we define the unit vectors $\hat{\zeta}'$ by

$$\hat{\zeta}' = N_-^{-1}((g_\perp A_\perp/2g - g_\mu\mu_\mu H)\sin\theta, 0, (g_{||}A_{||}/2g - g_\mu\mu_\mu H)\cos\theta) , \tag{A3}$$

where

$$g = [g_{||}^2\cos^2\theta + g_\perp^2\sin^2\theta]^{1/2} ,$$
$$N_- = \left[\left(\frac{g_{||}A_{||}}{2g} - g_\mu\mu_\mu H\right)^2\cos^2\theta + \left(\frac{g_\perp A_\perp}{2g} - g_\mu\mu_\mu H\right)^2\sin^2\theta\right]^{1/2} . \tag{A4}$$

Defining the spin-raising and spin-lowering operators relative to $\hat{\xi},\hat{\eta},\hat{\zeta}$ for the electron spin, and $\hat{\xi}',\hat{\eta}',\hat{\zeta}'$ for the muon spin, where $\hat{\xi}'$ and $\hat{\eta}'$ are perpendicular to $\hat{\zeta}'$ and to each other and $\hat{\eta}' = \hat{\eta}$, then Eq. (A2) can be written as

$$\mathcal{H} = g\mu_B H S_\xi + N_- I_{\zeta'} + K\cos\varphi_-(S_\xi - \tfrac{1}{2})I_{\zeta'} + \tfrac{1}{2}K\sin\varphi_-(S_\xi - \tfrac{1}{2})(I_+ + I_-)$$
$$+ \tfrac{1}{4}(N_1 - A_\perp)(S_+I_+ + S_-I_-) + \tfrac{1}{4}(N_1 + A_\perp)(S_+I_- + S_-I_+) + \tfrac{1}{2}N_2(S_+ + S_-)I_{\zeta'} . \tag{A5}$$

This form of the spin Hamiltonian is used to calculate the energies of the electron-spin-up states. The additional parameters in Eq. (A5) are

$$K=\frac{1}{g}(g_{\parallel}^2A_{\parallel}^2\cos^2\theta+g_{\perp}^2A_{\perp}^2\sin^2\theta)^{1/2}\ ,$$

$$\cos\varphi_-=N_-^{-1}\left[\tfrac{1}{2}K-\frac{g_\mu\mu_\mu H}{gK}(g_{\parallel}A_{\parallel}\cos^2\theta+g_{\perp}A_{\perp}\sin^2\theta)\right]\ ,$$

$$\sin\varphi_-=-\frac{g_\mu\mu_\mu H}{gKN_-}(g_{\perp}A_{\perp}-g_{\parallel}A_{\parallel})\sin\theta\cos\theta\ ,$$

$$N_1=N_-^{-1}\left[\tfrac{1}{2}A_{\parallel}A_{\perp}-\frac{1}{g}(g_{\parallel}A_{\perp}\cos^2\theta+g_{\perp}A_{\parallel}\sin^2\theta)g_\mu\mu_\mu H\right]\ ,$$

$$N_2=gN_-^{-1}\left[\frac{g_{\parallel}g_{\perp}}{2g}(A_{\perp}^2-A_{\parallel}^2)-(g_{\parallel}A_{\perp}-g_{\perp}A_{\parallel})g_\mu\mu_\mu H\right]\sin\theta\cos\theta\ . \tag{A6}$$

Solving the eigenvalue equation for the Hamiltonian of Eq. (A5) to third order for the upper two energy levels actually involves using some terms which appear in fourth-order perturbation theory. The energy difference between these two levels gives the frequency of one μSR line,

$$h\nu_{43}=N_--\frac{A_{\perp}N_1}{4g\mu_BH}-\frac{1}{16(g\mu_BH)^2}\left[(N_2^2-N_1^2-A_{\perp}^2)K\cos\varphi_-+2N_1N_2K\sin\varphi_-+2(N_1^2+A_{\perp}^2)N_--\frac{1}{2N_-}A_{\perp}^2N_2^2\right]\ . \tag{A7}$$

A similar analysis but using the muon quantization axis appropriate to $M_S=-\frac{1}{2}$ gives the result

$$h\nu_{21}=N_+-\frac{A_{\perp}N_3}{4g\mu_BH}+\frac{1}{16(g\mu_BH)^2}\left[(N_4^2-N_3^2-A_{\perp}^2)K\cos\varphi_++2N_3N_4K\sin\varphi_+-2(N_3^2+A_{\perp}^2)N_++\frac{1}{2N_+}A_{\perp}^2N_4^2\right]\ , \tag{A8}$$

where

$$N_+=\left[\left[\frac{g_{\parallel}A_{\parallel}}{2g}+g_\mu\mu_\mu H\right]^2\cos^2\theta+\left[\frac{g_{\perp}A_{\perp}}{2g}+g_\mu\mu_\mu H\right]\sin^2\theta\right]^{1/2}\ ,$$

$$\cos\varphi_+=-\frac{1}{N_+}\left[\tfrac{1}{2}K+\frac{g_\mu\mu_\mu H}{gK}(g_{\parallel}A_{\parallel}\cos^2\theta+g_{\perp}A_{\perp}\sin^2\theta)\right]\ ,$$

$$\sin\varphi_+=-\frac{g_\mu\mu_\mu H}{gKN_+}(g_{\perp}A_{\perp}-g_{\parallel}A_{\parallel})\sin\theta\cos\theta\ ,$$

$$N_3=-\frac{1}{N_+}\left[\tfrac{1}{2}A_{\parallel}A_{\perp}+\frac{1}{g}(g_{\parallel}A_{\perp}\cos^2\theta+g_{\perp}A_{\parallel}\sin^2\theta)g_\mu\mu_\mu H\right]\ ,$$

$$N_4=-\frac{1}{gN_+}\left[\frac{g_{\parallel}g_{\perp}}{2g}(A_{\perp}^2-A_{\parallel}^2)+(g_{\parallel}A_{\perp}-g_{\perp}A_{\parallel})g_\mu\mu_\mu H\right]\sin\theta\cos\theta\ . \tag{A9}$$

The frequency ν_{43} or ν_{21} will be lower depending on whether $A_{\parallel}+A_{\perp}$ is positive or negative, respectively. The lower of these is the one observed in the experiments described in this paper. It can be written in a particularly useful form providing that the anisotropy of the g factor is small and the field is close to the magic field. Equation (A7) or (A9), now just to second order, then becomes

$$h\nu=\tfrac{1}{4}|A_{\parallel}-A_{\perp}|+\frac{1}{2}\frac{g_\mu\mu_\mu}{g_0\mu_B}\frac{A_{\perp}|A_{\parallel}-A_{\perp}|}{A_{\parallel}+A_{\perp}}$$
$$+\frac{A_{\perp}^2-A_{\parallel}^2}{|A_{\perp}^2-A_{\parallel}^2|}\left[g_\mu\mu_\mu(H-H_M^{(1)})+\frac{1}{2}\frac{g_\mu\mu_\mu}{g_0\mu_B}\frac{A_{\perp}(A_{\parallel}+A_{\perp})}{|A_{\parallel}+A_{\perp}|}\right]\cos(2\theta)-\frac{1}{16}\frac{A_{\perp}^2-A_{\parallel}^2}{|A_{\perp}-A_{\parallel}|}\frac{\Delta g}{g_0}[1-\cos(4\theta)]\ , \tag{A10}$$

where

$$\Delta g=g_{\parallel}-g_{\perp}\ ,$$
$$g_0=\tfrac{1}{3}g_{\parallel}+\tfrac{2}{3}g_{\perp}\ , \tag{A11}$$
$$H_M^{(1)}=\frac{1}{4g_\mu\mu_\mu}|A_{\parallel}+A_{\perp}|\ .$$

[1]B. D. Patterson, A. Hintermann, W. Kündig, P. F. Meier, F. Waldner, H. Graf, E. Recknagel, A. Weidinger, and Th. Wichert, Phys. Rev. Lett. **40**, 1347 (1978); E. Holzschuh, W. Kündig, B. D. Patterson, H. Apel, J. P. F. Sellschop, and M. Stemmet, Phys. Rev. A **25**, 1272 (1982); E. Holzschuh, H. Graf, E. Recknagel, A. Weidinger, Th. Wichert, and P. F. Meier, Phys. Rev. B **20**, 4391 (1979).

[2]K. W. Blazey, T. L. Estle, E. Holzschuh, P. F. Meier, B. D. Patterson, and M. Richner, Hyperfine Interact. **17-19**, 595 (1984).

[3]T. L. Estle, M. E. Warren, and B. D. Patterson, Hyperfine Interact. **17-19**, 589 (1984); T. L. Estle, S. L. Rudaz, E. Holzschuh, R. F. Kiefl, B. D. Patterson, W. Kündig, and K. W. Blazey, Hyperfine Interact. **17-19**, 623 (1984).

[4]A. Hintermann, P. F. Meier, and B. D. Patterson, Am. J. Phys. **48**, 956 (1980).

[5]G. D. Watkins and J. W. Corbett, Phys. Rev. **121**, 1001 (1961).

[6]G. D. Watkins and J. W. Corbett, Phys. Rev. **134**, A1359 (1964).

[7]J. C. Philips, Comments Solid State Phys. **3**, 67 (1970).

[8]M. Lannoo and J. C. Bourgoin, Physica **116B**, 85 (1983).

[9]Y-H. Lee and J. W. Corbett, Phys. Rev. B **8**, 2810 (1973).

[10]E. G. Sieverts, Phys. Status Solidi B **120**, 11 (1983).

[11]R. F. Kiefl, J. W. Schneider, H. Keller, W. Kündig, W. Odermatt, B. D. Patterson, K. W. Blazey, T. L. Estle, and S. L. Rudaz, Phys. Rev. B **32**, 530 (1985).

[12]C. Boekema, E. Holzschuh, W. Kündig, P. F. Meier, B. D. Patterson, W. Reichart, and K. Rüegg, Hyperfine Interact. **8**, 401 (1981); E. Holzschuh, W. Kündig, and co-workers, Ref. 1.

[13]J. C. Phillips, *Bonds and Bands in Semiconductors* (Academic, New York, 1973).

[14]T. L. Estle, Hyperfine Interact. **17-19**, 585 (1984).

[15]J. Bernholc, N. O. Lipari, J. T. Pantalides, and M. Scheffler, Phys. Rev. B **26**, 5706 (1982).

[16]B. D. Patterson, A. Bosshard, D. Straumann, P. Truöl, A. Wüest, and Th. Wichert, Phys. Rev. Lett. **52**, 938 (1984).

[17]N. Sahoo, K. C. Mishra, and T. P. Das (private communication).

[18]A. Mainwood, A. M. Stoneham, T. L. Estle, and K. W. Blazey (private communication).

[19]J. A. Brown, R. H. Heffner, M. Leon, S. A. Dodds, T. L. Estle, and D. A. Vanderwater, Phys. Rev. B **27**, 3980 (1983).

[20]S. L. Rudaz, T. L. Estle, K. W. Blazey, B. D. Patterson, and W. Kündig, Bull. Am. Phys. Soc. **29**, 491 (1984).